

TIME-LAGGED T-DISTRIBUTED STOCHASTIC NEIGHBOR EMBEDDING (T-SNE) OF MOLECULAR SIMULATION TRAJECTORIES

A PREPRINT

Vojtěch Spiwok

Department of Biochemistry and Microbiology
University of Chemistry and Technology, Prague
Technická 5, Prague 6, 166 28, Czech Republic
spiwokv@vscht.cz

Pavel Kríž

Department of Mathematics
University of Chemistry and Technology, Prague
Technická 5, Prague 6, 166 28, Czech Republic
krizp@vscht.cz

March 6, 2020

ABSTRACT

Molecular simulation trajectories represent high-dimensional data. Such data can be visualized by methods of dimensionality reduction. Non-linear dimensionality reduction methods are likely to be more efficient than linear ones due to the fact that motions of atoms are non-linear. Here we test a popular non-linear t-distributed stochastic neighbor embedding (t-SNE) method on analysis of trajectories of alanine dipeptide dynamics and Trp-cage folding and unfolding. Furthermore, we introduced a time-lagged variant of t-SNE in order to focus on slow motions in the molecular system. This time-lagged t-SNE efficiently visualizes slow dynamics of molecular systems.

Keywords molecular dynamics · dimensionality reduction · trajectory analysis · tSNE

1 Introduction

The main goal of molecular simulations is identification of key states of studied systems and building of thermodynamic and kinetic models of transitions between these states. Identification of key states is often based on some numerical descriptors known as collective variables. Distance between two atoms can be seen as one of the simplest collective variables. It can be used, for example, to distinguish between the bound and unbound state in a simulation of protein-ligand interaction. For some more complex processes it is necessary to use more complex collective variables.

Collective variables are in fact dimensionality reduction methods because they represent high dimensional structure of a molecular system using few numerical descriptors. It is therefore no surprise that general linear and nonlinear dimensionality reduction methods have been applied on molecular simulation trajectories. Namely, principal component analysis [1], diffusion maps [2], sketch map [3, 4], Isomap [5, 6], autoencoders [7] or t-SNE [8, 9] have been tested in analysis of trajectories, data compression or sampling enhancement.

Advantage of nonlinear dimensionality reduction methods is their ability to describe more variance in data compared to linear methods with the same number of dimensions. This is especially true for t-distributed Stochastic Neighbour Embedding (t-SNE) [10]. This method became highly popular in many fields, including data science, bioinformatics and computational linguistics.

There are two features of t-SNE that contributed to its success. First, t-SNE converts high-dimensional points into low-dimensional points in a way to reproduce their proximity rather than distances. For example, for a bioinformatician analyzing genomic data to develop genomics-based diagnosis it is important that samples with the same diagnosis are close to each other after dimensionality reduction. It is unimportant how distant are samples with different diagnosis, provided that they are distant enough. Second, t-SNE unifies density of low-dimensional points in the output space. This feature, which can be controlled by a parameter called perplexity, makes visual representation of points more effective.

Disadvantage of application of general dimensionality reduction methods on molecular simulation trajectories is that these methods pick the most intensive (in terms of changes of atomic coordinates) motions in the system. However, such motions are often not interesting. Instead, for building of thermodynamic and kinetic models or to enhance sampling it is useful to extract slowest (i.e. energetically most demanding) motion. This can be done by Time-lagged Independent Component Analysis (TICA) [11, 12, 13]. TICA extracts slowest motions in the molecular system because it correlates the state of system with the state of the same system after a short delay (lag). This lag can be controlled.

Here we attempt to join advantages of t-SNE and TICA into a single method of time-lagged t-SNE. The method was tested on two molecular trajectories – on 200 ns simulation of alanine dipeptide and 208.8 μ s simulation of Trp-cage mini-protein folding and unfolding (trajectory kindly provided by DE Shaw Research)[14].

2 Methods

Time-lagged t-SNE is inspired by implementation of TICA using the AMUSE algorithm [15]. We start with atomic coordinates $\mathbf{X}(t)$ recorded over time t . First, coordinates are superimposed to a reference coordinates of the system to eliminate translational and rotational motions. After that, time-averaged coordinates are subtracted, leading to coordinates $\mathbf{X}'(t)$. Next, a covariance matrix is calculated as:

$$C_{ij}^{\mathbf{X}'} = \langle X'_i(t) X'_j(t) \rangle, \quad (1)$$

where i and j are indexes of atomic coordinates and $\langle \rangle$ denotes time-averaging. Next, covariance matrix is decomposed to eigenvalues $\lambda^{\mathbf{X}'}$ (the square matrix with eigenvalues on diagonal and zeros elsewhere) and eigenvectors $\mathbf{W}^{\mathbf{X}'}$ (the matrix with eigenvectors as columns):

$$\mathbf{C}^{\mathbf{X}'} \mathbf{W}^{\mathbf{X}'} = \mathbf{W}^{\mathbf{X}'} \lambda^{\mathbf{X}'}. \quad (2)$$

Coordinates $\mathbf{X}'(t)$ are transformed onto principal components and normalized by roots of eigenvalues (space-whitening the signal):

$$\mathbf{Y}(t) = (\lambda^{\mathbf{X}'})^{-1/2} ((\mathbf{W}^{\mathbf{X}'})^T \mathbf{X}'(t)). \quad (3)$$

A time-lagged covariance matrix is calculated as:

$$C_{ij}^{\mathbf{Y}} = \langle Y_i(t) Y_j(t + \tau) \rangle, \quad (4)$$

where τ is an adjustable time lag. Because the matrix \mathbf{C} is non-symmetric it must be symmetrized as:

$$\mathbf{C}_{sym}^{\mathbf{Y}} = 1/2(\mathbf{C}^{\mathbf{Y}} + (\mathbf{C}^{\mathbf{Y}})^T). \quad (5)$$

Next, this symmetric matrix is decomposed to eigenvalues $\lambda^{\mathbf{Y}}$ and eigenvectors $\mathbf{W}^{\mathbf{Y}}$:

$$\mathbf{C}_{sym}^{\mathbf{Y}} \mathbf{W}^{\mathbf{Y}} = \mathbf{W}^{\mathbf{Y}} \lambda^{\mathbf{Y}}. \quad (6)$$

Finally, $\mathbf{Y}(t)$ are transformed onto principal components and expanded by eigenvalues:

$$\mathbf{Z} = \lambda^{\mathbf{Y}} ((\mathbf{W}^{\mathbf{Y}})^T \mathbf{Y}). \quad (7)$$

This step expands distances in directions with highest autocorrelations, which represent directions with slow motions.

It is possible to use certain number of eigenvectors with highest eigenvalues instead of all eigenvectors. t-SNE can be applied on distances between simulation snapshots calculated in the space of \mathbf{Z} as:

$$D_{t,t'} = \|\mathbf{Z}(t) - \mathbf{Z}(t')\|. \quad (8)$$

All analyses were done by programs written in Python with MDtraj [16], PyEMMA [17], numpy [18] and scikit-learn [19] libraries. It is available at GitHub (<https://github.com/spiwokv/tltsne>) and using PyPI.

The trajectory of alanine dipeptide was obtained by unbiased 200 ns molecular dynamics simulation of a system containing alanine dipeptide and 874 water molecules in Gromacs [20]. It was modelled by Amber99SB-ILDN force field [21]. Electrostatic interactions were treated by particle-mesh Ewald method [22]. Temperature was kept constant by V-rescale thermostat [23].

The trajectory of Trp-cage folding and unfolding was kindly provided by DE Shaw Research.

3 Results

The method was tested on two molecular systems – on alanine dipeptide and Trp-cage. In order to test time-lagged t-SNE we compare time-lagged t-SNE with standard t-SNE and TICA.

3.1 Alanine Dipeptide

Time-lagged t-SNE was first applied on a trajectory of alanine dipeptide without water and hydrogen atoms. It is important to remove hydrogen atoms because rotamers of methyl groups by approx. 120 deg are mathematically distinguishable but chemically identical. The trajectory was sampled every 20 ps (10,001 snapshots). Time lag τ was set to 3 frames (60 ps). The value of perplexity was set to 3.0 and Euclidean space was used to calculate the distance matrix D .

The value of lag time was chosen based on TICA results. Similar calculations with lag time set to 1 to 12 steps show that lag time set to 1-7 works well on a simple system such as alanine dipeptide (see Supplementary Material).

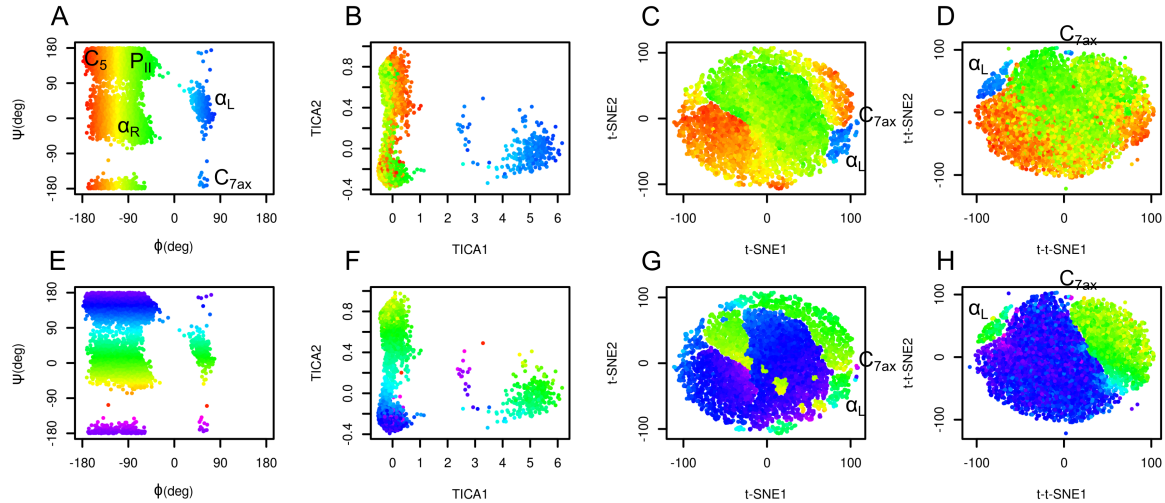


Figure 1: Time-lagged t-SNE (t-t-SNE) applied on 200 ns simulation of alanine dipeptide in water. Conformations sampled in the simulations were projected into the space of Ramachandran torsions ϕ and ψ (A, E), TICA coordinates (B, F), t-SNE (C, G) and time-lagged t-SNE (D, H). Points are colored by Ramachandran torsion ϕ (A-D) and ψ (E-H).

The results are depicted in Figure 1. Plots in the space of Ramachandran torsions show that all relevant conformations of alanine dipeptide were sampled. Plots in the space of TICA coordinates show that rotation around ϕ is the slowest and rotation around ψ is the second slowest motion in the studied system.

Plots in the space of t-SNE coordinates has a yin-and-yang-like shape. These plots show a limitation of conventional t-SNE, which is an improper resolution of conformations. Namely, there are several yellow-green islands in the blue area of the plot colored by ϕ values (G).

Time-lagged t-SNE (t-t-SNE) does not suffer this problem. The blue area in the plot generated by time-lagged tSNE is continuous and does not contain any islands of conformations with positive ϕ values (H). This can be explained by the fact that introduction of a time lag into t-SNE causes higher separation of key conformations of alanine dipeptide.

One feature is common to the original t-SNE as well as our time-lagged variant. This is the fact that t-SNE flattens the distribution of points in the output space. This results into almost uniform distribution of points in each minimum.

It is possible to calculate a histogram of some molecular collective variable or collective variables and convert it into a free energy surface. Most common interpretation of such free energy surface is that deep minima correspond to stable states whereas shallow minima correspond to unstable states. This approach can be applied for conventional descriptors, such as Ramachandran angles of alanine dipeptide. However, due to flattening of distribution of points by t-SNE or by time-lagged t-SNE such free energy surface is relatively flat. Populations of different states can be calculated from areas of free energy minima rather than from their depths.

3.2 Trp-cage

t-SNE and time-lagged t-SNE analysis was performed on the trajectory of Trp-cage folding and unfolding sampled every 20 ns (10,440 snapshots). Lag time was set to three frames (60 ns). Perplexity was set to 10.0.

Similarly to alanine dipeptide, lag time was chosen based on TICA analysis. Comparison of embeddings calculated for lag time set to 1, 2, 3, 4, 5, 10, 15 and 20 (in number of frames) shows that lag time 1 to 5 works well.

Initial analysis by time-lagged t-SNE resulted into a circular plot with multiple points located outside clusters of points on the edges of the circle. This indicates that there are many points with high distances $D_{t,t'}$. In order to eliminate these points we reduced the number of eigenvectors \mathbf{W}^Y to top 50 eigenvectors (option `-maxpcs` in the code).

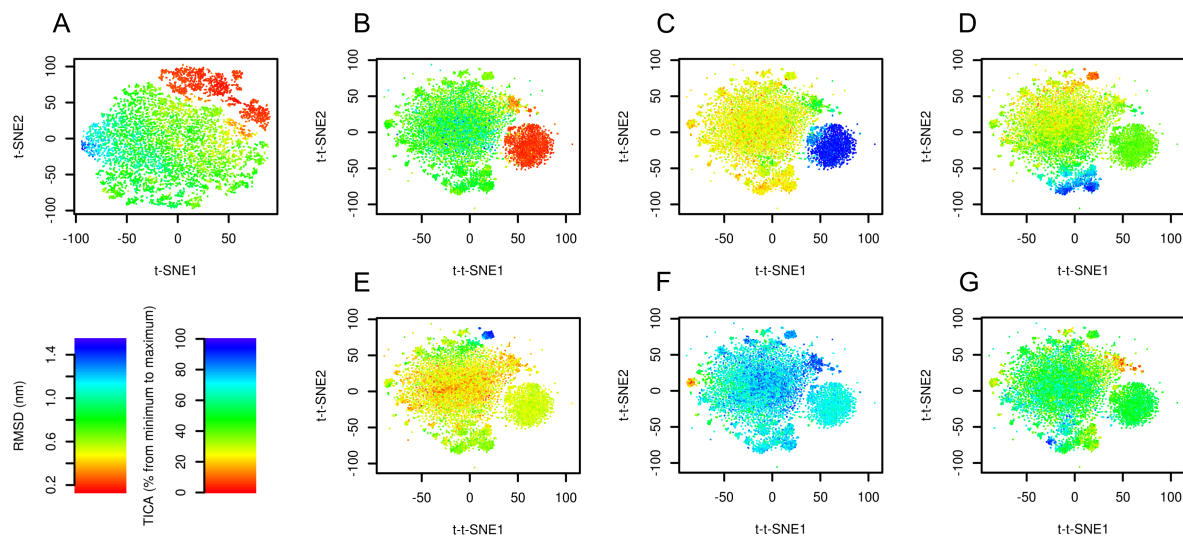


Figure 2: Time-lagged t-SNE (t-t-SNE) applied on 208.8 μ s of Trp-cage folding and unfolding. The trajectory was analysed by t-SNE (A) and time-lagged t-SNE (B-G). Points are colored by RMSD from the native structure (A, B) and by the first (C), second (D), third (E), fourth (F) and fifth (G) TICA coordinate.

The results are depicted in Figure 2. Figure 2A shows the trajectory analysed by conventional t-SNE colored by RMSD from the native structure (PDB ID: 112y). There is clear relationship between t-SNE coordinates, in particular t-SNE1, and RMSD. The native structure (in red) forms a cluster in top right corner of the plot. Structures with high RMSD (in blue) are characterized by lowest values of t-SNE1.

The trajectory analysed by time-lagged t-SNE colored by RMSD is depicted in Figure 2B. Similarly to Figure 2A the native structure forms a distinct cluster. In contrast to the conventional t-SNE, structures with high values of RMSD are scattered in the large cluster in the center. This indicates that transitions between high-RMSD structures are fast.

Figures 2C-G show same plots colored by TICA coordinates. The first TICA coordinate (Figure 2C) distinguishes folded and unfolded structures. Plots colored by other TICA coordinates (Figures 2D-G) show usually a red or blue clusters on edges of the plot. This shows that time-lagged t-SNE captures slowest motions characterized by TICA, but more efficiently than TICA itself, because these motions can be depicted in a single plot.

Figures 2D, F and G show clusters with opposite values of TICA coordinates (red vs. blue) on opposite sites of plots. The interpretation is that conformations with slow mutual transitions are located on distant locations in the plot.

Figure 3 shows representative structures of Trp-cage from the simulation trajectory projected onto time-lagged t-SNE embeddings. Structure 1 is the native structure. Structure 2 is a known near-native structure. Structures 3-6 were

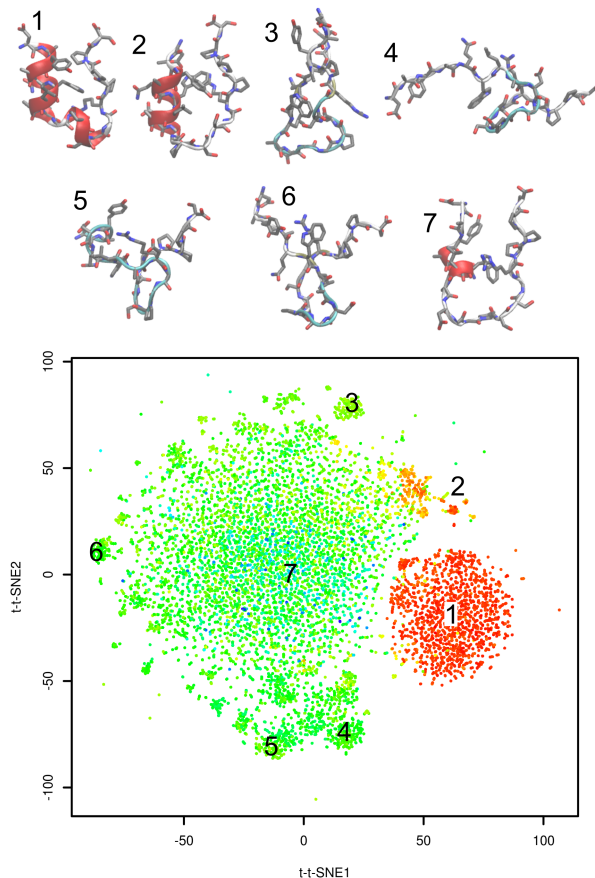


Figure 3: Representative structures projected onto time-lagged t-SNE embeddings. Plot is colored by RMSD from the native structure (as in Fig. 2B).

sampled from clusters on peripheral areas of time-lagged t-SNE embeddings. Finally, structure 7 was taken from the middle of the plot. Visual inspection indicates that structures 3-6 may be kinetic traps of Trp-cage folding, because these structures are characterized by formation of numerous non-native hydrogen bonds and other interactions. Also the near-native structure 2 is likely to be a kinetic trap of Trp-cage folding.

4 Discussion

Choice of lag time for time-lagged t-SNE was driven by TICA analysis. Values of 3 frames (60 ps, 0.03 % of the whole trajectory) for alanine dipeptide and 3 frames (60 ns, 0.029 % of the whole trajectory) for Trp-cage led to visually plausible low dimensional embeddings. This indicates, that 0.03 % of trajectory size is good initial choice of lag time.

As an alternative to time-lagged t-SNE it is possible to use time-lagged autoencoders recently reported by Wehmeyer and Noé [25]. Autoencoders are feed-forward neural networks with an hourglass-like architecture. The input signal (atomic coordinates or other features) from the input layer are transformed via hidden layers into the central bottleneck layer. Next, the signal from the bottleneck layer are transformed via another hidden layers into the output layers. Parameters of the network are trained to obtain agreement between the input and output signal. The signal in the bottleneck layer represents a non-linear low-dimensional representation of the input signal. Unlike classical autoencoders, time-lagged autoencoders focus on slowest motions, not on the most intensive motions [25].

The clear advantage of autoencoders and their time-lagged variant is the possibility to calculate low-dimensional embeddings for a new out-of-sample structure. Extensive testing of time-lagged autoencoders in the original article [25] was possible owing to this fact. Time-lagged autoencoders can be trained on a training set and tested on a validation set, i.e. they can be evaluated by cross-validation. Furthermore, they can be trained on a small training set and then applied on a large set of input data. This is efficient since the training part is in general significantly more expensive than the

calculation of embeddings on out-of-sample structures. Time-lagged autoencoders are useful for pre-processing of structural data for building of Markov state models.

There are limited options for calculation of t-SNE low-dimensional embeddings for out-of-sample structures. Therefore, t-SNE and time-lagged t-SNE are not suitable for pre-processing of the structural data. We see the advantage of time-lagged t-SNE (similarly to t-SNE) in visualization.

Time-lagged t-SNE in the current implementation also cannot be used as collective variables in simulations using bias force or bias potential because these methods require on-the-fly calculation of low-dimensional embeddings and their derivatives with respect to atomic coordinates. However, there are tools to approximate such low-dimensional embeddings [6, 26].

One of key features of t-SNE is that it can reconstruct proximities and not distances in the low-dimensional output space. In time-lagged t-SNE this means that states separated by low energy barriers are close to each other. States separated by large energy barriers are far from each other, but time-lagged t-SNE does not attempt to preserve their distances accurately. This means that two close points in the time-lagged t-SNE plot can be connected by an energetically favorable path.

Another key feature of t-SNE is perplexity and the fact that t-SNE flattens the distribution of points in the output space. This is useful for visualization. For this reason t-SNE (as well as time-lagged t-SNE) must be used with caution as a pre-processing for calculation of free energy surfaces and for clustering. t-SNE can also create artificial cluster when perplexity is not set properly.

5 Acknowledgement

This work was funded by COST action OpenMultiMed (CA15120, Ministry of Education, Youth and Sports of the Czech Republic LTC18074) and Czech National Infrastructure for Biological Data (ELIXIR CZ, Ministry of Education, Youth and Sports of the Czech Republic LM2015047). Authors would like to thank D. E. Shaw Research for data used in this work.

References

- [1] A. Amadei, A. B. Linssen and H. J. Berendsen Essential dynamics of proteins. *Proteins*. 1993, 17(4):412–25.
- [2] A. L. Ferguson, A. Z. Panagiotopoulos, P. G. Debenedetti and I. G. Kevrekidis Systematic determination of order parameters for chain dynamics using diffusion maps. *Proc. Natl. Acad. Sci. USA* 2010, 107(31):13597–13602 doi: 10.1073/pnas.1003293107
- [3] M. Ceriotti, G. A. Tribello and M. Parrinello Simplifying the representation of complex free-energy landscapes using sketch-map. *Proc. Natl. Acad. Sci. USA* 2011, 108(32):13023–13028. doi: 10.1073/pnas.1108486108
- [4] G. A. Tribello, M. Ceriotti and M. Parrinello Using sketch-map coordinates to analyze and bias molecular dynamics simulations. *Proc. Natl. Acad. Sci. USA* 2012, 109(14):5196–5201 doi: 10.1073/pnas.1201152109
- [5] P. Das, M. Moll, H. Stamati, L. E. Kavraki and C. Clementi Low-dimensional, free-energy landscapes of protein-folding reactions by nonlinear dimensionality reduction *Proc. Natl. Acad. Sci. USA* 2006, 103(26):9885–9890. doi: 10.1073/pnas.0603553103
- [6] V. Spiwok and B. Králová Metadynamics in the conformational space nonlinearly dimensionally reduced by Isomap *J. Chem. Phys.* 2011, 135, 224504 doi: 10.1063/1.3660208
- [7] W. Chen and A. L. Ferguson Molecular enhanced sampling with autoencoders: on-the-fly collective variable discovery and accelerated free energy landscape exploration. *J. Comput. Chem.* 2018, 39, 2079–2102. doi: 10.1002/jcc.25520
- [8] M. Duan, J. Fan, M. Li, L. Han and S. Huo Evaluation of dimensionality-reduction methods from peptide folding-unfolding simulations. *J. Chem. Theory Comput.* 2013, 9:2490–2497. doi: 10.1021/ct400052y
- [9] G. A. Tribello and P. Gasparotto Using dimensionality reduction to analyze protein trajectories *Front. Mol. Biosci.* 2019, 6:46 doi: 10.3389/fmolb.2019.00046
- [10] L. J. P. van der Maaten and G. E. Hinton Visualizing high-dimensional data using t-SNE. *J. Mach. Learn. Res.* 2008, 9:2579–2605.
- [11] L. Molgedey and H. G. Schuster Separation of a mixture of independent signals using time delayed correlations. *Phys. Rev. Lett.* 1994, 72, 3634–3637.

- [12] G. Perez-Hernandez, F. Paul, T. Giorgino, G. de Fabritiis and F. Noé Identification of slow molecular order parameters for Markov model construction. *J. Chem. Phys.* 2013, 139, 015102.
- [13] C. R. Schwantes and V. S. Pande Improvements in Markov state model construction reveal many non-native interactions in the folding of NTL9. *J. Chem. Theory Comput.* 2013, 9, 2000–2009.
- [14] K. Lindorff-Larsen, S. Piana, R. O. Dror and D. A. Shaw How fast-folding proteins fold. *Science*. 2011, 334, 517–520. doi: 10.1126/science.1208351
- [15] A. Hyvarinen, J. Karhunen and E. Oja Independent component analysis. 2001, John Wiley & Sons Int.
- [16] R. T. McGibbon, K. A. Beauchamp, M. P. Harrigan, C. Klein, J. M. Swails, C. X. Hernández, C. R. Schwantes, L.-P. Wang, T. J. Lane and V. S. Pande MDTraj: A modern open library for the analysis of molecular dynamics trajectories *Biophys. J.*, 2015, 109(8):1528–1532. doi: 10.1016/j.bpj.2015.08.015
- [17] C. Wehmeyer, M. K. Scherer, T. Hempel, B. E. Husic, S. Olsson, F. Noé Introduction to Markov state modeling with the PyEMMA software. *Living J. Comp. Mol. Sci.* 2019, 1(1):5965. doi: 10.33011/livecoms.1.1.5965
- [18] T. E. Oliphant A Guide to NumPy. 2006, Spanish Fork, UT: Trelgol Publishing.
- [19] F. Pedregosa, G. Varoquaux, A. Gramfort, V. Michel, B. Thirion, O. Grisel, M. Blondel, P. Prettenhofer, R. Weiss, V. Dubourg, J. Vanderplas, A. Passos, D. Cournapeau, M. Brucher, M. Perrot and E. Duchesnay Scikit-learn: Machine learning in Python. *J. Mach. Learn. Res.* 2011, 12:2825–2830.
- [20] M. J. Abraham, T. Murtola, R. Schulz, S. Páll, J. C. Smith, B. Hess, E. Lindahl GROMACS: High performance molecular simulations through multi-level parallelism from laptops to supercomputers *SoftwareX* 2015, 1-2:19–25. doi: 10.1016/j.softx.2015.06.001
- [21] K. Lindorff-Larsen, S. Piana, K. Palmo, P. Maragakis, J. L. Klepeis, R. O. Dror and D. E. Shaw Improved side-chain torsion potentials for the Amber ff99SB protein force field. *Proteins* 2010, 78(8):1950–1958. doi: 10.1002/prot.22711
- [22] T. Darden, D. York and L. Pedersen Particle mesh Ewald: An $N \cdot \log(N)$ method for Ewald sums in large systems. *J. Chem. Phys.* 1998, 98(12):10089. doi: 10.1063/1.464397
- [23] G. Bussi, D. Donadio and M. Parrinello Canonical sampling through velocity-rescaling. *J. Chem. Phys.* 2007, 126:014101.
- [24] M. M. Sultan and V. S. Pande Automated design of collective variables using supervised machine learning. *J. Chem. Phys.* 2018, 149:094106. doi: 10.1063/1.5029972
- [25] C. Wehmeyer and F. Noé Time-lagged autoencoders: deep learning of slow collective variables for molecular kinetics. *J. Chem. Phys.* 2018, 148:241703. doi: 10.1063/1.5011399
- [26] D. Trapl, I. Horvancanin, V. Mareska, F. Ozcelik, G. Unal and V. Spiwok Anncolvar: Approximation of complex collective variables by artificial neural networks for analysis and biasing of molecular simulations. *Front. Mol. Biosci.* 2019, 6:25. doi: 10.3389/fmolb.2019.00025

TIME-LAGGED T-DISTRIBUTED STOCHASTIC NEIGHBOR EMBEDDING (T-SNE) OF MOLECULAR SIMULATION TRAJECTORIES

A PREPRINT

Vojtěch Spiwok

Department of Biochemistry and Microbiology
University of Chemistry and Technology, Prague
Technická 5, Prague 6, 166 28, Czech Republic
spiwokv@vscht.cz

Pavel Kříž

Department of Mathematics
University of Chemistry and Technology, Prague
Technická 5, Prague 6, 166 28, Czech Republic
krizp@vscht.cz

March 6, 2020

1 Supplementary Material

Supplementary figures Fig. S1, Fig. S2 and Fig. S3.

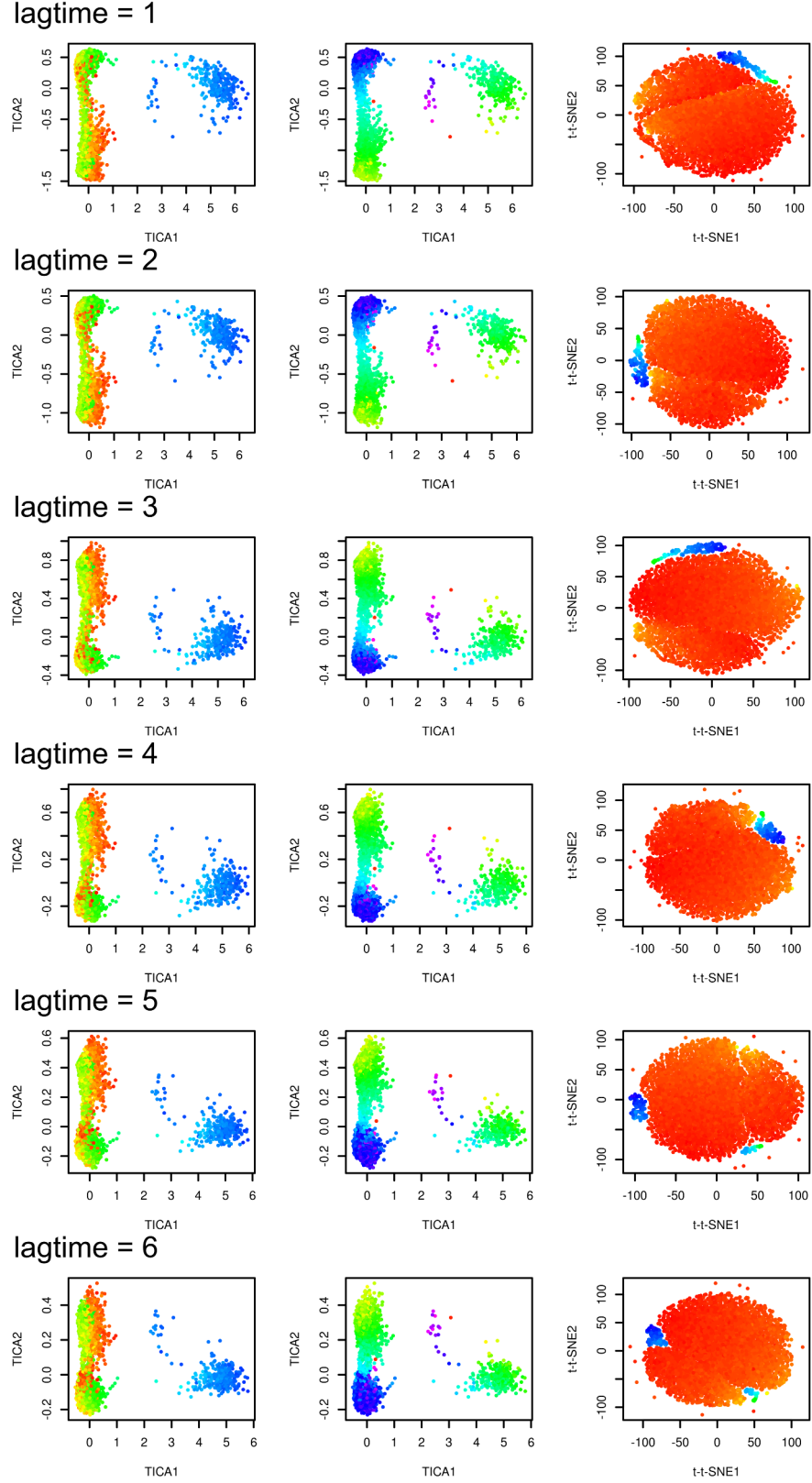


Figure S1: Effect of lag time on time-lagged t-SNE of alanine dipeptide trajectory. TICA plots are colored by ϕ (left) and ψ (centre, as in Fig. 1). Time-lagged t-SNE plots are colored by the first TICA coordinate (as in Fig. 1).

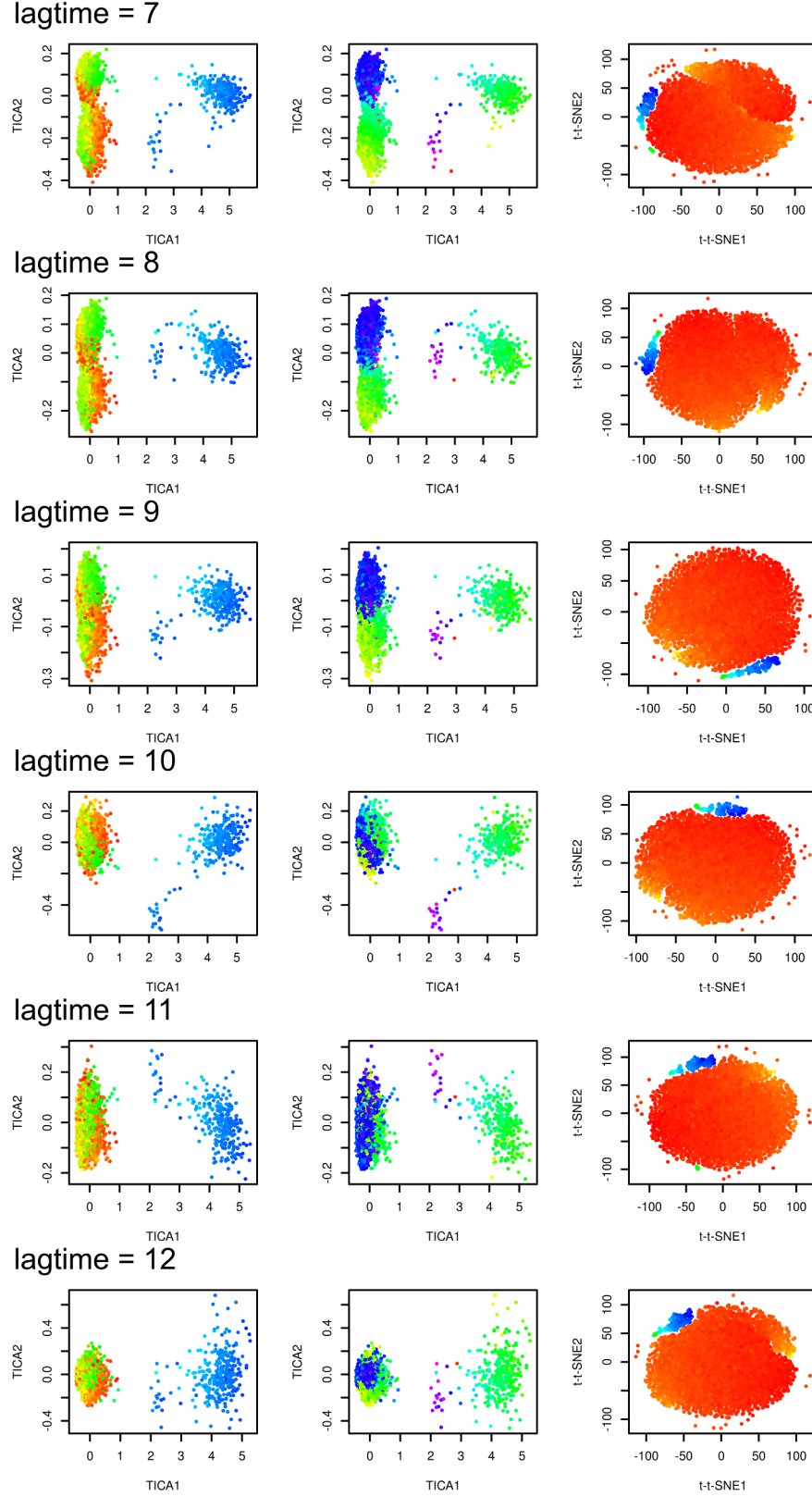


Figure S2: Effect of lag time on time-lagged t-SNE of alanine dipeptide trajectory. TICA plots are colored by ϕ (left) and ψ (centre, as in Fig. 1). Time-lagged t-SNE plots are colored by the first TICA coordinate (as in Fig. 1).

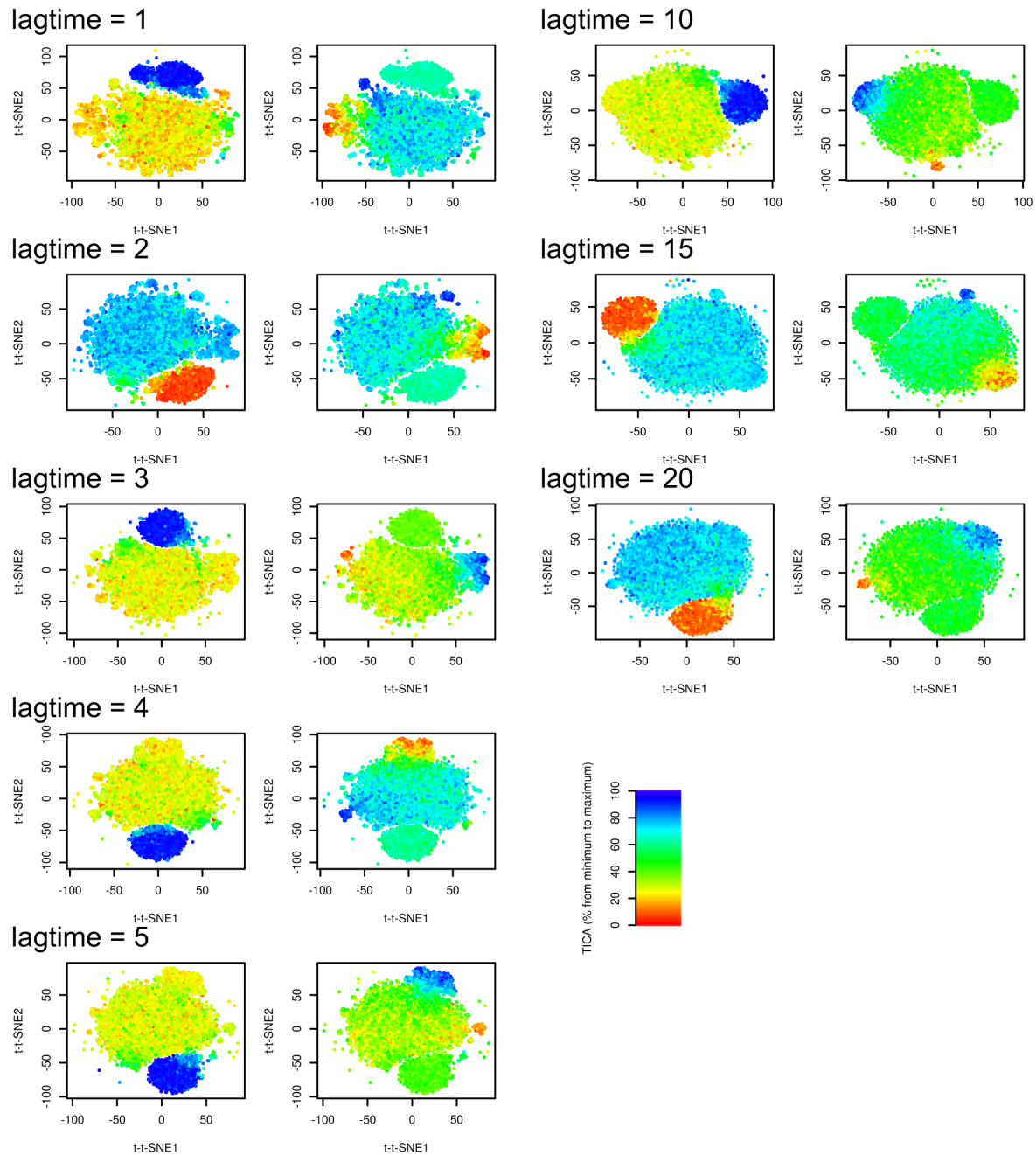


Figure S3: Effect of lag time on time-lagged t-SNE of Trp-cage folding trajectory. Plots are colored by the first and the second TICA coordinate (left and right, respectively).